

**SEISMIC CAT SCAN OF AN ANCIENT  
EARTHQUAKE ALONG THE  
OQUIRRH FAULT,  
UTAH**

by

David M. Morey

A thesis submitted to the faculty of  
The University of Utah  
in partial fulfillment of the requirements for the degree of

Master of Science

in

Geophysics

Department of Geology and Geophysics

The University of Utah

March 1998

Copyright © David M. Morey 1998  
All Rights Reserved





## ABSTRACT

Two-dimensional (2-D) and three-dimensional seismic (3-D) surveys were conducted across the Oquirrh fault, of Northern Utah with the purpose of imaging the fault related structure to a depth of 40-60 ft. The scientific objective was to use the resulting reflectivity and tomographic images to deduce the paleoseismic history of this fault zone. The tomographic images were generated by conducting a seismic CAT (computer axial tomography) scan of the fault zone by inverting first-arrival traveltimes of 3-D seismic data.

The 3-D seismic data (112,896 traces) were collected over a 145 ft x 30 ft patch of ground along the Oquirrh fault. Their first arrival traveltimes were then picked and inverted by a 3-D tomographic technique. To complement the 3-D tomogram, a 2-D reflectivity image was obtained by a 570 ft long reflection survey that cut across the fault. Results show that the 3-D tomogram clearly delineates the fault and a colluvial wedge, both of which correlate well with the geologic cross-section taken from the adjacent trench. The thickness of the colluvial-wedge image provided an estimate of 22.8 ft for the surface displacement of the last surface-rupturing event on the Oquirrh fault. This thickness measurement was also used with the layer dip angles measured from the 2-D reflectivity section to give a moment magnitude estimate of 6.8 for the most recent earthquake. This is in very good agreement with the magnitude estimate of 7.0 based on a nearby trenching study.

This study demonstrates that seismic imaging methods can clearly delineate the shape and depth of a colluvial wedge associated with a normal fault earthquake. It also shows that information from reflectivity images and tomographic images can be combined to accurately estimate the size of prehistoric earthquakes. It is conjectured that a wider recording aperture could have enabled the imaging of multiple colluvial wedges at depth, and so provided the necessary information to estimate recurrence

intervals of large magnitude earthquakes. This assumes that the timing of the colluvial wedge formation can be obtained by dating of cores drilled through the wedges. Thus, a useful tool in paleoseismology is established where 3-D tomography combined with 2-D reflection imaging has the possibility of providing deeper and wider, but less resolved, images of fault systems than the excavation of trenches across faults. In some cases, this may provide a viable alternative to the intrusive task of fault trenching.

To my parents

# CONTENTS

<b>ABSTRACT</b> .....	<b>iv</b>
<b>LIST OF FIGURES</b> .....	<b>x</b>
<b>ACKNOWLEDGMENTS</b> .....	<b>xii</b>
<b>1. INTRODUCTION</b> .....	<b>1</b>
1.1 Purpose and Scope .....	1
1.2 Site Geology .....	1
1.3 Survey Location .....	5
1.4 Previous Seismic Imaging of Shallow Fault Zones .....	5
1.5 Oquirrh Fault Imaging .....	7
1.6 Organization of the Thesis .....	8
<b>2. OQUIRRH FAULT IMAGING EXPERIMENT DESIGN</b> .....	<b>9</b>
2.1 2-D Seismic Survey .....	9
2.2 3-D Seismic Survey .....	11
<b>3. DATA PROCESSING</b> .....	<b>15</b>
3.1 Refraction Processing .....	15
3.1.1 3-D Traveltime Algorithm .....	15
3.1.2 Quality Control of Traveltime Picks .....	18
3.1.3 Synthetic Tomography Results .....	20
3.2 2-D CDP Reflection Processing .....	24
3.2.1 Theoretical Resolution Limits .....	25
3.2.2 Data Sorting .....	26
3.2.3 Automatic Gain Control .....	28
3.2.4 Shot and Receiver Statics .....	28
3.2.5 Common Midpoint Sorting and Muting .....	31
3.2.6 Velocity Analysis .....	31
3.2.7 Residual Statics .....	35
3.2.8 Poststack Migration .....	37
<b>4. RESULTS OF OQUIRRH FAULT IMAGING</b> .....	<b>42</b>
4.1 Reflection Results .....	42
4.2 Tomography Results .....	45



<b>5. INTERPRETATION</b> .....	<b>58</b>
5.1 Measuring Displacement From The Colluvial Wedge . . . . .	58
5.2 Calculating Net Vertical Tectonic Displacement . . . . .	59
5.3 Calculating Paleoearthquake Magnitude . . . . .	62
5.3.1 Calculating Paleoearthquake Magnitude From Displacement .	62
5.3.2 Calculating Paleoearthquake Magnitude From Surface Rupture Length . . . . .	64
5.3.3 Calculating Paleoearthquake Magnitude From Displacement and Surface Rupture Length . . . . .	65
<b>CONCLUSIONS</b> .....	<b>67</b>
<b>REFERENCES</b> .....	<b>69</b>

## LIST OF FIGURES

1	Map of Utah and the northern section of the Oquirrh fault. The dashed lines in the lower left figure define the boundaries of major geologic provinces and the stars indicate the location and magnitude of major earthquakes. . . . .	2
2	Log interpretation showing the shallow geology adjacent to the Oquirrh fault (Olig et al., 1996). . . . .	4
3	Cross-section of main fault zone in Trench BC-3 (Olig et al., 1996). The colluvial wedge is the result of rapid deposition following a surface rupturing earthquake and is a reliable indicator of a large magnitude event. . . . .	6
4	Eastward aerial view of survey location and trench excavated by the UGS. The approximate location of the 2-D and 3-D surveys are indicated, where the 3-D survey encompasses an area of 145 ft x 30 ft. . .	7
5	Shows the extent of the 2-D seismic line in relation to the trenching study (Olig et al., 1996) conducted by the UGS. The vertical exaggeration is 6.5:1. . . . .	10
6	Source locations on 3-D grid, where "*" correspond to station locations and the solid lines correspond to relative elevation contours (feet). . .	12
7	Receiver locations denoted by "*" on the 3-D grid for (top) first patch of geophones and (bottom) second patch of geophones. . . . .	13
8	Common shot gather for a shot at station 20 and all inline receivers along crossline 4. The trace interval is 1.5 ft. . . . .	14
9	Plot of RMS residual vs iteration number. The large drop in RMS residual after iteration number 8 is caused by refining the grid from $dx = 2'$ to $dx = 1'$ . . . . .	19
10	Reciprocity test. Dashed line represents first arrival times, $t(i, j)$ for the $i$ th stationary shot point and the $j$ th receiver location. Solid line represents the first arrival times for $t(j, i)$ . Most of the above travel times satisfy the reciprocity test, i.e. $t(i, j) = t(j, i)$ to within a tolerance of $\pm 6$ ms. . . . .	20
11	3-D reciprocity test. Plot of discrepancy times $ t(i,j) - t(j,i) $ that exceeded 6 ms vs the receiver offset. . . . .	21
12	Comparison of first-arrival traveltimes for two shots in the same position following a cable shift. The maximum separation of the two lines is less than 2.5 ms which is below the estimated picking error. . . . .	22

13	Checkerboard test results: comparison of the upper 40 ft of (top) a slice of the 3-D tomogram, (middle) the model, and (bottom) the 2-D tomogram. The 3-D tomogram appears to have fewer artifacts than the 2-D tomogram at the 25-30 ft levels. . . . .	23
14	Raypath density image associated with the 3-D checkerboard test. This shows that rays penetrated to a depth of about 40 feet for this shooting geometry and velocity gradient. . . . .	24
15	X-Z slice of the raypath coverage for the 3-D tomographic result sliced at $y = 15ft$ . Compare with Figure 16 and notice the increased ray coverage for the 3-D result. . . . .	25
16	Raypath coverage for the 2-D tomographic result. Compare with Figure 15. . . . .	26
17	Chart of the CDP processing flow for the Oquirrh fault 2-D data. . .	27
18	Common shot gather for a shot at station 30 with AGC applied and a trace spacing of 3 ft. The data are dominated by ground roll at the far offset traces. . . . .	29
19	Common offset gather for an offset of 9 ft. The arrow indicates the air wave, which should be flattened after a shot statics correction. . . . .	30
20	Raw CMP 179 with a trace interval of 1.5 ft. . . . .	32
21	CMP 179 after muting to be compared with Figure 20. . . . .	33
22	Semblance panels for CMP 250 (left) and 650 (right) where the CMP interval is 0.75 ft. Darker areas correspond to larger semblance values and, typically, better stacking velocities. The solid line indicates the estimated velocity profile for that CMP. . . . .	34
23	Velocity analysis of the stacked seismic section with CMPs between 100-150 (top) and 400-450 (bottom). The reflectors appear to be most coherent at stacking velocities of 1000 ft/s (top) and 1150 ft/s (bottom). . . . .	36
24	Contour plot of the velocities used to produce the final stacked section. Contours are in ft/s. . . . .	37
25	Comparison of a CMP with a NMO correction applied before (left) and after (right) maximum energy stacking. The reflection events appear more "flat" in the CMP with maximum energy stacking. . . . .	38
26	Comparison of a portion of the stacked section with (top) and without (bottom) maximum energy stacking. Notice the improved coherency of reflectors in the rectangles in the bottom figure. See Figure 5 for the ground locations associated with CMP values. . . . .	39
27	Migrated section (top) and stacked seismic section (bottom). The migrated section provides a more accurate dip estimate of the subsurface horizons. The CMP interval is 0.75 ft. . . . .	41
28	The final migrated section with the horizontal axis in CMP and the vertical axis in depth. . . . .	43

29	Simplified cross-section from trench BC-3, after Olig et al. (1996). The vertical exaggeration is 6.5:1. . . . .	44
30	Zoom view of the reflectivity image of the antithetic fault. Notice the thickening and sloping of horizons 1-4 as they approach the antithetic fault. . . . .	46
31	Common offset gather for an offset of 30 ft and the final stacked section, where the times in the common offset gather have been adjusted for topography. Key features are indicated by arrows and described in the text. . . . .	47
32	3-D velocity tomogram computed from the traveltimes picked from the 3-D data. Note the wedge shaped low velocity region associated with the colluvial wedge. . . . .	48
33	Comparison of the geologic cross-section (Olig et al., 1996) and the equivalent portion of the 3-D tomogram. Notice the strong correlation between both figures in the location and shape of the colluvial wedge. . . . .	50
34	Horizontal slice of 3-D tomogram at Z=33 ft. Notice the velocity depression (LVZ 2) that runs parallel to the fault and the velocity depression LVZ 1 that corresponds to the colluvial wedge. LVZ 2 is interpreted in the trench log as a channel. . . . .	51
35	X-Z slice of the 3-D velocity tomogram sliced at y=10 ft. The colluvial wedge is clearly identified in the figure and is characterized by a low velocity. . . . .	52
36	X-Z slice of the 3-D velocity tomogram sliced at y=15 ft. . . . .	53
37	X-Z slice of the 3-D velocity tomogram sliced at y=20 ft. . . . .	54
38	Comparison of 2-D vs 3-D tomograms. The colluvial wedge is more clearly defined in the 3-D tomogram (bottom) than in the 2-D tomogram (top). . . . .	55
39	Images of raypaths showing areas that were visited by at least 500 rays. . . . .	56
40	Comparison of the 3-D tomogram and the final stacked section. The colluvial wedge is clearly imaged in the tomogram, but its presence in the stacked section is ambiguous. . . . .	57
41	Image of the colluvial wedge showing where the maximum thickness was measured. . . . .	60
42	The components required for calculating net vertical tectonic displacement ( $T_{net}$ ). The components are displacement ( $T_m$ ), tilt displacement ( $T_t$ ) over a certain distance ( $W$ ), and vertical displacement on the antithetic fault ( $T_a$ ). . . . .	61
43	The amount of dip on horizon 1 is measured outside the graben at location A and inside the graben at B to define the amount of tilt due to faulting. Offset on the antithetic fault was measured at location C. . . . .	63

## ACKNOWLEDGMENTS

I would like to thank my adviser Gerard Schuster for his knowledge and his patience to share it with me. I have learned many lessons from Dr. Schuster during my stay at the University of Utah, many in the classroom and many on the basketball court. Dr. Schuster is a dedicated and hard working geophysicist who has extensive knowledge on the subject and the creativity to always be a leader in the field. I am proud to have worked with Dr. Schuster. Thanks Jerry! Thanks are also offered to the members of my advisory committee, Bob Smith and Marjorie Chan, for reviewing this manuscript. Bob Smith and Art Sylvester sparked my interest in geophysics. I will always remember working in the Tetons and Yellowstone. Special thanks go to Dr. Ron Bruhn for sharing his ideas on this project and his evaluation of the results.

I would like to thank my parents for the years of support along this journey. They have given me the solid foundation that has made it possible for me to come this far. My wife has been along my side for the duration of this project, she has provided the love and support that have made this possible. She has always been patient on those late nights necessary to complete this project.

Thank you to all those who helped in the collection of this data. Jing Chen, Zhaojun Liu, Fanlin Meng, Hougchuan Sun, Yue Wang, and Chengjun Wu worked many hard, long hours during this process. I benefited from financial support administered by the Department of Geology and Geophysics (Chevron Fellowship), the College of Mines (Dougan Fellowship), and the Society of Exploration Geophysicists. Finally I would like to thank the 1996 and 1997 members of the UTAM project for their financial support.

# 1. INTRODUCTION

## 1.1 Purpose and Scope

The purpose of this thesis research is to reconstruct the shallow structure ( $0 < Z < 150$  ft) of the Oquirrh fault zone, Northern Utah, with two-dimensional (2-D) and three-dimensional (3-D) seismic imaging techniques and use these images to deduce the paleoseismic history of the fault. The 3-D survey is over a 145 ft x 30 ft patch of ground, whereas the 2-D seismic survey is a single line of length 570 ft. The imaging techniques are common midpoint (CMP) reflection stacking, poststack migration and travelttime tomography. The target body is a colluvial wedge system along the Oquirrh fault scarp. The colluvial wedge is the product of a large surface normal faulting event and can give information about the event that produced it. For example, the size of the colluvial wedge can give information on the magnitude of the event (Ostenaar, 1984); and the number of multiple wedges can provide information on the recurrence interval for surface rupturing events on the fault (Keaton, 1993). Trenching studies suggest that this normal fault erupts every 13,300 to 22,100 yrs with a magnitude 7.0 or larger earthquake (Olig et al., 1996). This study uses seismic imaging to probe deeper than the 10-ft deep trench and gain additional information on the size, geometry, and recurrence interval of earthquakes on the Oquirrh fault. The implication of this work suggest that seismic imaging methods can complement or even replace many trenching studies in paleoseismology.

## 1.2 Site Geology

The Oquirrh Fault zone lies at the western base of the Oquirrh Mountains, east Tooele County, Utah (Soloman, 1996). A west-dipping normal fault, the Oquirrh Fault is located at the eastern extent of the Basin and Range extensional province. The fault zone shown in Figure 1 extends for about 21 km from Lake Point to just

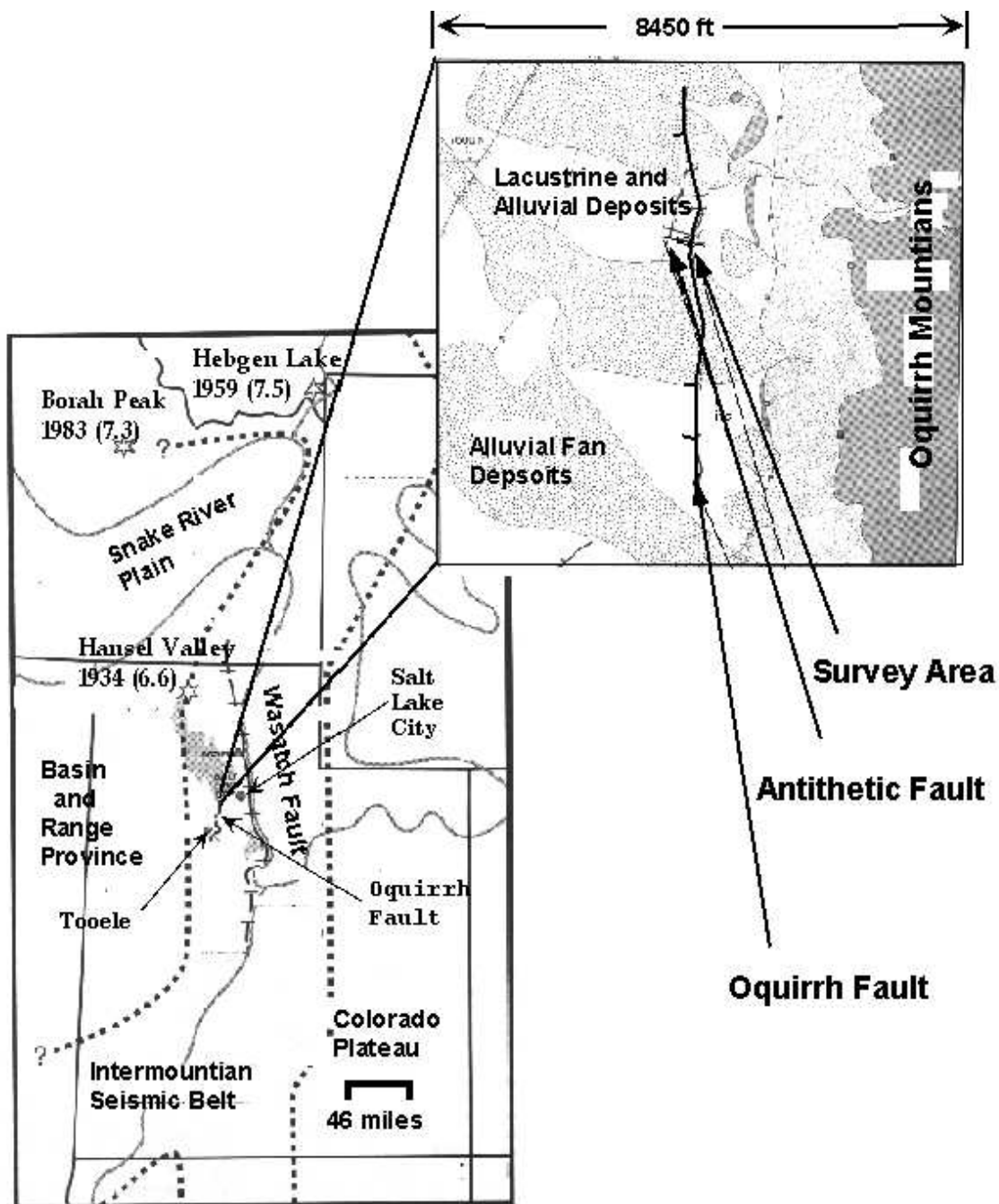


Figure 1: Map of Utah and the northern section of the Oquirrh fault. The dashed lines in the lower left figure define the boundaries of major geologic provinces and the stars indicate the location and magnitude of major earthquakes.

south of Tooele, Utah, and lies about 35 km west of the Wasatch Fault zone which is the most active Quaternary fault in Utah and marks the eastern boundary of the Basin and Range extensional province (Machette et al., 1991). The Oquirrh fault is also located within the Intermountain Seismic Belt (Smith and Sbar, 1974; Smith and Arabasz, 1991) and has not experienced a historic earthquake since 1847 (Olig et al., 1996). Seismicity in the Intermountain Seismic Belt and well-bore breakouts along the Wasatch front indicate that extension is still occurring in the west-northwest to west direction (Zoback, 1983, 1989; Eddington et al., 1987; Bjornadottir and Pechmann, 1989). This suggests that the area is subject to future large earthquakes threatening the communities of Tooele and Salt Lake City and the Tooele Army Depot.

Faulting along the Oquirrh fault was first recognized by geomorphologist G.K. Gilbert in July 1880: "Approaching Tooele there is a fine view of the fault scarp in the embayment of the mts (mountains)" (Hunt, 1982, p. 170). Deposition in the area of the Oquirrh fault has been dominated by alluvial-fan sediments shed from the Oquirrh Mountains to the east and paleolake deposited lacustrine sediments (Soloman et al., 1992). The Tooele Valley, bounded on the east by the Oquirrh fault, was repeatedly inundated by paleolakes in the late Quaternary (Olig et al., 1996). Lake Bonneville produced three distinct shorelines in the Tooele Valley: the Stansbury, Bonneville, and Provo in chronological order. These two depositional environments (alluvial and lacustrine) produce the surficial geology in the northern section of the Oquirrh fault zone. The lacustrine sediments form a thin mantle ( 3 ft) over older alluvium and are buried by the most recent alluvial-fan deposition (Olig et al., 1996). Bedrock outcrops in the Oquirrh Mountains to the east with the Rogers Canyon Nappe (Soloman, 1996).

A trenching study (Olig et al., 1996) on the Oquirrh fault penetrated to a depth of about 12 ft and revealed the shallow geology. The strata adjacent to the fault is shown in Figure 2 and is characterized by colluvium overlaying fault-scarp colluvium, debris-flow deposits, shallow- to deep-water lacustrine deposits, shallow-water lacustrine deposits, and transgressive beach deposits in order of increasing depth (Olig et al., 1996).



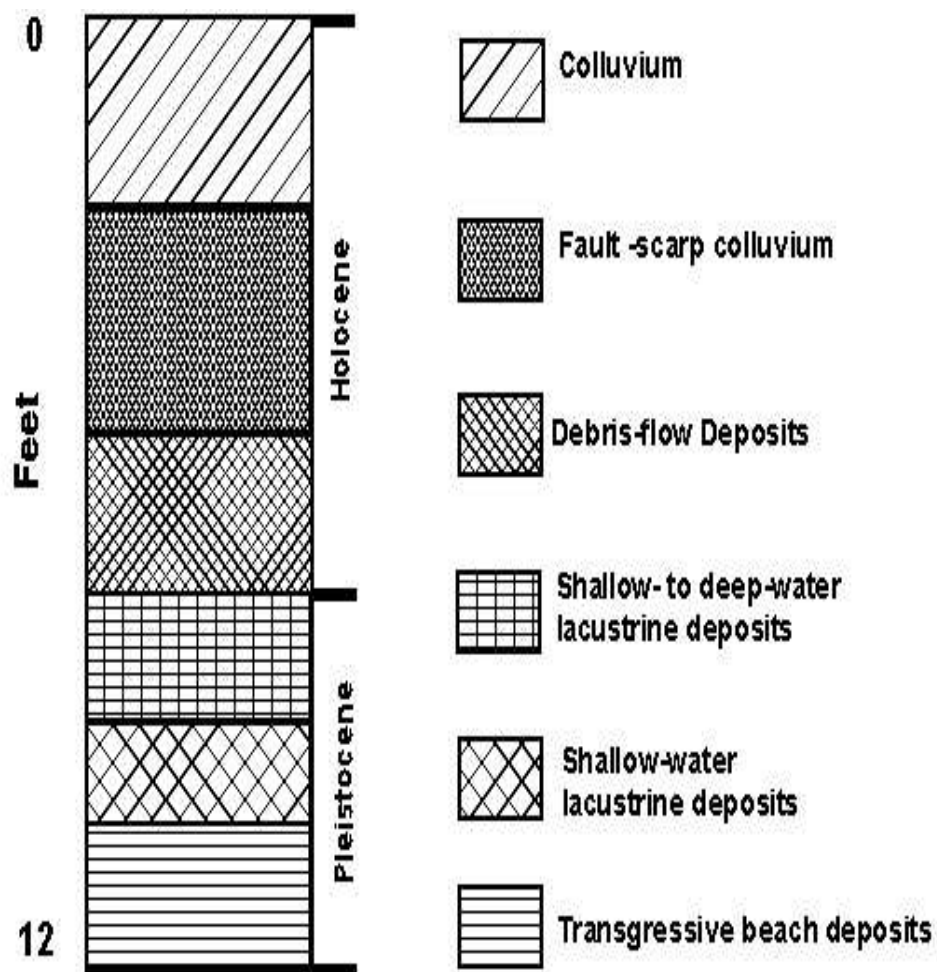


Figure 2: Log interpretation showing the shallow geology adjacent to the Oquirrh fault (Olig et al., 1996).

The trenching study exposed a 2.2 m thick colluvial wedge associated with the most recent surface rupturing event (Olig et al., 1996). A paleoseismic study on the fault yielded an age estimate for this event between  $4340 \pm 60$  yrs. B.P. to  $7650 \pm 90$  yrs. B.P. and gave a recurrence estimate of 13,300-22,100 yrs (Olig et al., 1996). These dates were obtained by radiocarbon dating of faulted and unfaulted horizons in the trench. However, there is some uncertainty in these dates due to the inability of the trenching study to reveal multiple colluvial wedges. This is attributed to the shallow penetration of the trenches.

### **1.3 Survey Location**

University of Utah personnel conducted seismic surveys over the northern part of the Oquirrh Fault zone adjacent to a trench excavated across the fault by the Utah Geological Survey (UGS) near the mouth of Big Canyon (see Figures 3 and 4).

Figure 1 shows a map of the Northern Oquirrh fault and indicates the location of the trench and the 2-D and 3-D seismic surveys. The site was located approximately 2 km southeast of Lake Point, Utah, and 0.3 km west of Big Canyon (Figure 1). This location was selected for several reasons: first, the availability of detailed geologic information from the adjacent trench; second, the Quaternary geology of the area is reasonably well-known; third, the combination of alluvial and lacustrine deposits in the area should provide measurable seismic reflections. Finally, the Oquirrh fault has not received as much attention as the more famous faults in the Intermountain Region even though the fault is 30 km west of Salt Lake City and 7 km east of the Tooele Army Depot.

### **1.4 Previous Seismic Imaging of Shallow Fault Zones**

Investigating shallow fault zones with seismic techniques has been used for several years (Treadway et al., 1988; Miller et al., 1986; Ali et al., 1991). The majority of these investigations have used reflection methods to image the fault zone reflectivity providing information on the location and offset of the fault being investigated (Pratt

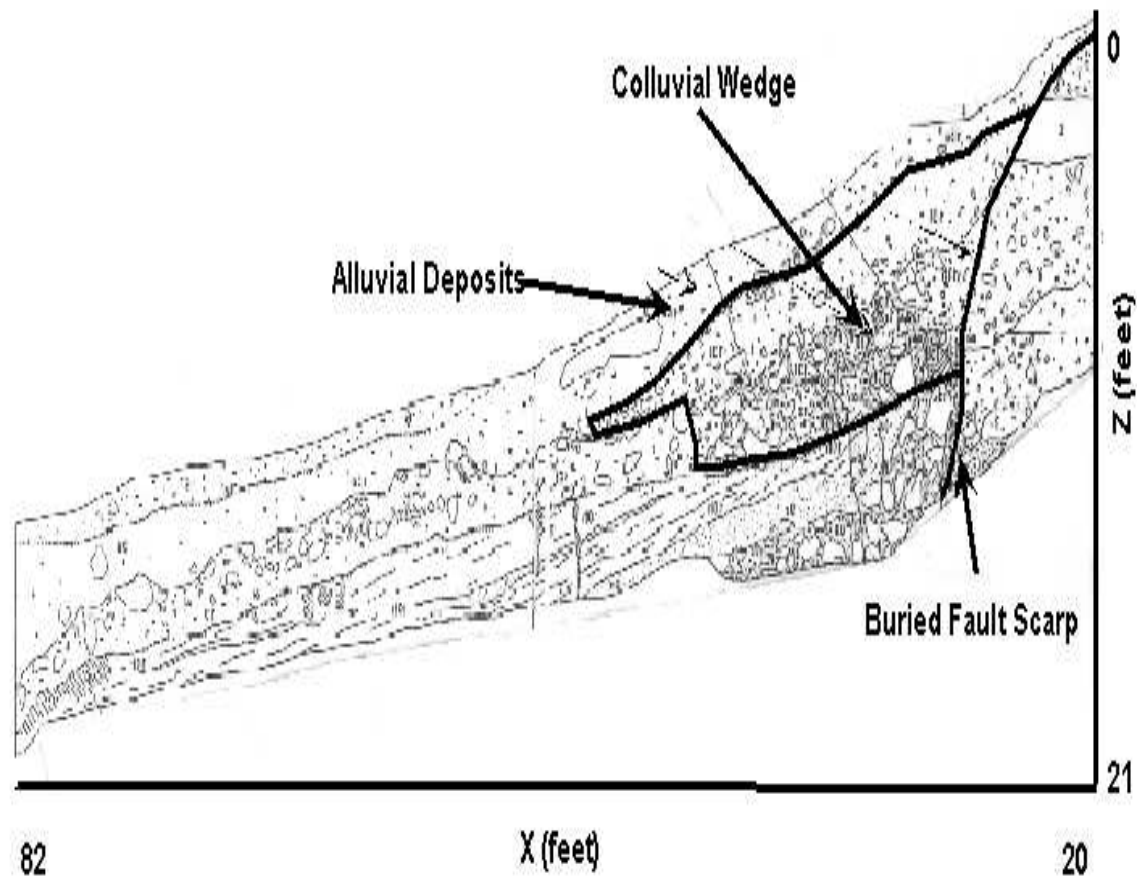


Figure 3: Cross-section of main fault zone in Trench BC-3 (Olig et al., 1996). The colluvial wedge is the result of rapid deposition following a surface rupturing earthquake and is a reliable indicator of a large magnitude event.

et al., 1997; Odem et al., 1997). Problems arise in this method because shallow reflections are difficult to collect due to a variety of problems including statics, strong surface waves, and poor signal-to-noise ratios (Louis and Karastathis, 1996). Thus, obtaining paleoseismic information on a shallow fault zone using seismic techniques can be a difficult task.

As an example, seismic investigations have been conducted on the Wasatch Fault (Stephenson, 1991) and the West Valley Fault (Keaton, 1993) which are in the Intermountain Seismic Belt and within 30 km of the Oquirrh fault. Both of these investigations were able to identify the location of the fault indicated by offsets in subsurface horizons, but the identification of colluvial wedges was ambiguous. Thus,

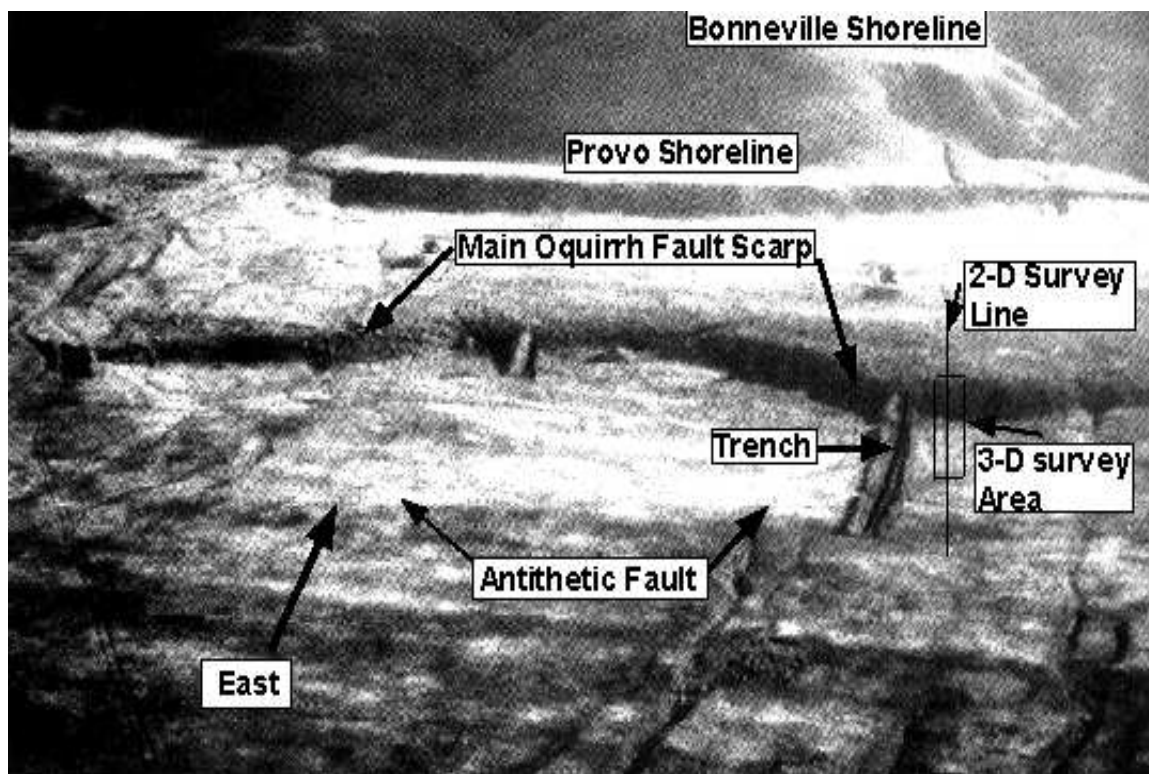


Figure 4: Eastward aerial view of survey location and trench excavated by the UGS. The approximate location of the 2-D and 3-D surveys are indicated, where the 3-D survey encompasses an area of 145 ft x 30 ft.

irrefutable paleoseismic information was not obtained. The shallow reflection events were polluted by near-surface scattering, surface-waves, and static shifts and so prevented the clear imaging of the colluvial wedge.

## 1.5 Oquirrh Fault Imaging

To overcome the problems with statics, near-surface scattering, and coherent noise, I use a refraction travelt ime tomography method as well as common depth point (CDP) reflection methods to provide information about the fault zone. The refraction arrivals are almost never obscured by random or coherent noise, so the refraction traveltimes can be picked with little error. I also use 3-D tomographic imaging to provide a more complete image of the fault, including lateral velocity variations along the fault. This technique offers greater confidence in the interpretation because the horizons are laterally continuous in three dimensions.

To collect the data for tomography, University of Utah personnel conducted 2-D and 3-D seismic surveys over a portion of the Oquirrh fault in May 1996 and May 1997 (see Figure 4). The data were collected on a fine grid in order to image the shallow ( $0 < z < 150$  ft) detailed features of this fault using 2-D reflection imaging and 3-D travelttime tomography. The 2-D data set consists of one seismic line that is 570 ft long and intersects the center of the 3-D survey grid. The 3-D survey covers a 145 ft x 30 ft patch of ground adjacent to a trench excavated by the UGS. This trench clearly reveals detailed geologic features of the Oquirrh fault over a vertical interval of 10 ft, and so it gives a calibration model for our reconstructed reflection and velocity images.

Processing of the seismic data includes 2-D reflection processing along with 2-D and 3-D tomography. The results are compared to the geologic cross-section (Figure 3) taken from the UGS trench.

## **1.6 Organization of the Thesis**

This thesis, whose goal is to develop paleoseismic imaging methods, is organized into five sections. Section 1 is the introduction and Section 2 contains information on data acquisition. Section 3 describes the processing of the data, and the fourth section contains the seismic and velocity images along with their interpretation. The final section contains the conclusions.